STUDIES ON VISUAL PERCEPTION
FOR PERCEPTUAL ROBOTICS

Özer Ciftcioglu, Michael S. Bittermann, I. Sevil Sariyildiz

Department of Building Technology, Delft University of Technology, Berlageweg 1, 2628 CR Delft, The Netherlands
o.ciftcioglu@tudelft.nl, m.s.bittermann@tudelft.nl, i.s.sariyildiz@tudelft.nl

Keywords: Visual perception, perception modeling, perception measurement, robotics, genetic search

Abstract: Studies on human visual perception measurement for perceptual robotics are described. The visual perception is mathematically modelled as a probabilistic process obtaining and interpreting visual data from an environment. The measurement involves visual openness perception in virtual reality, which has direct implications for navigation issues of actual autonomous robotics. The perception is quantified by means of a mapping function which converts a distance to an elemental perception estimate. The measurement is carried out with the averaging of the elemental perceptions in real time. This is accomplished by means of exponential averaging. The mapping function parameters are optimized uniquely by means of genetic algorithm approach where the data set for model development consists of a number of perception data samples. These are obtained from individuals who are confronted with a number of scenes and asked for their perceptual openness statements. Based on this data, a perception model is developed for a virtual robot where the simulated vision interaction of the robot with the environment is converted to visual openness estimation through the model output. The model outcome is essential visual information for the navigation of an autonomous perceptual robot.

1 INTRODUCTION

Robot navigation is one of the major fields of study in autonomous robotics (Beetz et al., 2001, Wang and Liu, 2004). As data source for navigation a number of approaches have been proposed. For instance video image processing (Florczyk, 2005), or obtaining distances between robot and its environment by means of ultrasonic sensors (Oriolio et al., 1998), infrared (Song and Cho, 2000), or via 3D laser (Surmann et al., 2001). In this work, the simulated laser approach is considered and implemented in a virtual reality (VR) environment. Being peculiar to this specific research, in place of merely measuring the distances between the robot and its environment, the robot's perception about its environment as to visual openness is considered. From the architectural design viewpoint, visual openness is an important concept in architecture and interior design. Since the shape of a space is responsible for the perception of an observer, visual openness is attributed as an inherent quality to the space. From the robotics viewpoint, visual openness perception is characteristic information about the environment and therefore can be used for the

human-like navigation of an autonomous perceptual robot.

In the present work, a virtual robot is used as a representative of a human, who moves through a space making continuous visual openness assessment about the environment for building technological design purposes. This assessment also can form a base of navigation information for path planning to make the robot autonomous with human-like visual openness assessments along the path it determines and moves.

2 PERCEPTION MODEL DEVELOPMENT

2.1 Theoretical Considerations

The subject matter of this work is visual openness perception which has essential implications on general design process as well as robot movement. The visual openness perception is obtained from visual perception data, which are derived from the

distances between observer and environment. That is, the visual openness of a space is perceived in mind with the association of the distances. This association is represented in this work by means of a sigmoid function.

The variation of sigmoid with the independent variable is shown in figure 1. The sigmoid function is a special function which is also used to represent biological processes. One important application is found in the paradigm of artificial neural networks, where sigmoid plays the essential role in modeling the non-linearity of a biological neuron.
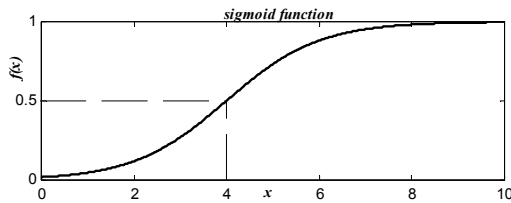

Figure 1: Sigmoid function $f(x) = 1/[1 + \exp(x - x_o)]$ which represents non-linearity in brain processes.

The characteristic behavior of the function is its saturation at the extremities and its approximately linear behavior in the middle range. Since such functionality can be surmised to occur in each neuron in the brain, the modeling of visual openness perception by such a function is a prominent choice among other options potentially available. Qualitatively, by means of the sigmoid function the perception of the visual openness at small distances is considered to be small with no significant change in this fuzzy range. A similar behavior is observed at the other extreme considering that the visual openness perception does not deviate significantly as the distance approaches to extreme values. At the middle range, the visual openness perception is highly dependent on the distance, as one should expect. These qualitative observations about the perception model are similar to many other biological processes of a human and they conform to the common visual openness perception experience of a human, in general.

Another interesting feature of sigmoid is that it is used to measure the perception quantitatively in the range between 0 and 1. This is a very significant feature especially while the robot is experiencing and evaluating the visual openness of a space as a fuzzy statement. Such statements can be statistically analyzed to establish the visual openness perception model parameters.

For the visual openness perception measurement we use the laser option, where the length of each visual ray between human eye and an object in the environment is represented by a laser ray spanning the ray source and the object. The distance is used to measure the visual openness perception. In this case, the laser source provides rays not in scanning mode but as a random source of rays with certain statistical properties, which are derived below. A number of rays are traced in this way and consequently the same amount of perception data is obtained. That is for each particular ray an elemental visual openness perception is obtained via a sigmoid function. By averaging these individual mapping function outcomes, the visual openness perception, as a measurement outcome, is obtained. The averaging is performed on a sample by sample basis so that the time-dependent measurement can be accomplished in real-time. If the time constant of the exponential averaging is kept sufficiently small then the measurement outcome can be used for robot navigation due to minimal latency of the measurement. In the case of a moving robot, it experiences human-like interaction with the environment.

For the visual openness perception model development and the analysis of the role of the sigmoid function, which maps the physical distance to visual openness perception, we start with the basics of the perception process with a simple yet fundamental geometry. This is shown in figure 2.
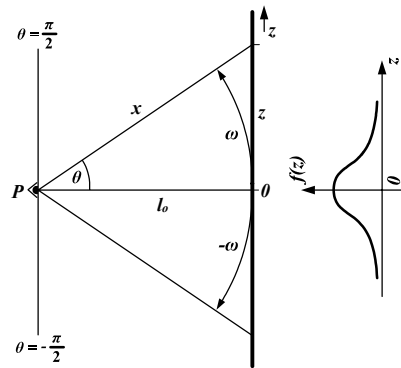

Figure 2: The geometry of visual perception from a top view where P represents the position of eye, looking at a vertical plane with a distance l_o to the eye; $f_z(z)$ is the probability density function of the perception.

In figure 2, the observer is facing and looking at a vertical plane from the point denoted by P. By means of looking action the observer pays visual attention equally to all directions within the scope of sight. That is, at the first instance, the observer visually experiences all regions of the plane without any preference for one region over another. Each location on the plane has its own distance within the

observer's scope of sight which is represented as a cone. The cone has a solid angle denoted by θ. The distance of a point on the plane and the observer is denoted by x and the distance between the observer and the plane is denoted by l_o. Since the visual perception is determined via the associated distances, it is straightforward to proceed to express the distance of visual perception in terms of θ. From figure 2, this is given by

$$x = \frac{l_o}{\cos(\theta)} \tag{1}$$

Since we consider the observer pays visual attention equally for all directions within the scope of sight in the first instance, the probability density function (pdf), which is associated with the directions, is uniformly distributed. Consequently, assuming the scope of sight is defined by the angle $\theta = \pi/4$, the pdf f_θ is given by

$$f_\theta = \frac{1}{\pi/2} \tag{2}$$

Since θ is a random variable, the distance x in (1) is also a random variable. The pdf $f_x(x)$ of this random variable is computed as follows.

Theorem on the *function of random variable*: To find $f_x(x)$ for a given x we solve the equation

$$x = g(\theta) \tag{3}$$

for θ in terms of x. If θ_1, θ_2,...., θ_n, .. are all its *real* roots, $x = g(\theta_1) = g(\theta_2) = ... = g(\theta_n) = ...$
Then

$$f_x(x) = \frac{f_\theta(\theta_1)}{|g'(\theta_1)|} + ... + \frac{f_\theta(\theta_2)}{|g'(\theta_2)|} + ... + \frac{f_x(\theta_n)}{|g'(\theta_n)|} + .. \tag{4}$$

Clearly, the numbers θ_1, θ_2,...., θ_n, .. depend on x. If, for a certain x, the equation $x = g(\theta)$ has no real roots, then $f_x(x) = 0$.
According the theorem above,

$$g'(\theta) = \frac{dx}{d\theta} = \frac{l_o \sin(\theta)}{\cos^2(\theta)} \tag{5}$$

Between $\theta = -\pi/4$ and $\theta = +\pi/4$,

$$g(\theta) = \frac{l_o}{\cos(\theta)} \tag{6}$$

has two roots, which are equal and given by

$$\theta_{1,2} = \arccos(\frac{l_o}{x}) \tag{7}$$

Using (7) in (5), we obtain

$$g'(\theta) = \frac{x\sqrt{x^2 - l_o^2}}{l_o} \tag{8}$$

Substituting (2), (7) and (8) into (4), we obtain

$$f_x(x) = \frac{4}{\pi} \frac{l_o}{x\sqrt{x^2 - l_o^2}} \tag{9}$$

for the interval $l_o \leq x \leq \dfrac{l_o}{\cos(\pi/4)}$. For this interval, the integration below becomes

$$\int_{l_o}^{\sqrt{2}\,l_o} f_x(x)\,dx = \frac{4}{\pi} \int_{l_o}^{\sqrt{2}\,l_o} l_o \frac{dx}{x\sqrt{x^2 - l_o^2}} = 1 \tag{10}$$

as it should be as a pdf. The sketch of $f_x(x)$ vs x is given in figure 3 (upper) and its variation for $l_o = 1$ is also given in the same figure (lower). In place of a plane geometry, for a circular geometry, the pdf $f_x(x)$ in (9) takes a uniform distribution, as it is shown in the Appendix.
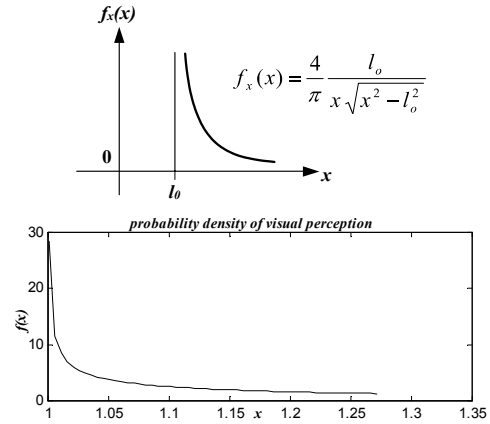

Figure 3: Variation of the probability density of random variable x representing the distance between eye and a location on a plane shown in figure 1. The upper plot is a sketch; the lower one is a computed plot with $l_o = 1$.

It is interesting to note that for the plane geometry in figure 2, the visual perception is sharply concentrated close to $x = l_o$ or $\theta \cong 0$, that is in perpendicular direction to the plane. This striking result is in conformity with the common human experience as to visual perception. Namely, for this geometry the visual perception is strongest along the axis of the cone of sight relative to the side directions. To see this in mathematical terms, we extend our calculations to derive the pdf along the z direction in figure 2. In this case, proceeding in the same way before, we write

$$tg(\theta) = \frac{z}{l_o} \quad (11)$$

$$z = g(\theta) = l_o\, tg(\theta)$$

$$g'(\theta) = \frac{dz}{d\theta} = \frac{l_o}{\cos^2(\theta)} = l_o(i + tg^2(\theta)) = l_o(1 + \frac{z^2}{l_o^2}) \quad (12)$$

$$\theta_1 = arctg(z/l_o)$$

$$f_z(z) = \frac{f_\theta(\theta_1)}{|g'(\theta_1)|} = \frac{l_o}{\pi(l_o^2 + z^2)} \quad (13)$$

for the interval $-\infty \leq z \leq \infty$. For this interval, the integration below becomes

$$\int_{-\infty}^{+\infty} f_z(z)\, dz = \frac{l_o}{\pi} \int_{-\infty}^{+\infty} \frac{dz}{z^2 + l_o^2} = 1$$

as it should be. The variation of $f_z(z)$ is shown in figure 2. This result clearly explains the relative importance of the front view as compared to side views in human visual perception. In the visual perception measurement system, $f_z(z)$ is taken close to a Gaussian function, for computational convenience. The implication of this approximation to the exact $f_x(x)$ given by (9) is presented below. From figure 2, we can write

$$x^2 = l_o^2 + z^2 \quad (14)$$

where

$$f_z(z) = \frac{1}{\sqrt{2\pi\sigma^2}} e^{-\frac{1}{2\sigma^2}z^2} \quad (15)$$

From (14), we write $z^2 = x^2 - l_o^2$, so that

$$z_{1,2} = \pm\sqrt{x^2 - l_o^2} \quad (16)$$

$$g(z) = \sqrt{l_o^2 + z^2} \quad (17)$$

$$g'(z) = \frac{dg}{dz} = \frac{1}{\sqrt{\left(\frac{l_o}{z}\right)^2 + 1}} \quad (18)$$

Substituting $z_{1,2}$ from (16) into (18) yields

$$g'(z_{1,2}) = \frac{1}{\sqrt{\frac{l_o^2}{x^2 - l_o^2} + 1}} \quad (19)$$

From the function of a random variable theorem

$$f_x(x) = \frac{f_z(z_1)}{|g'(z_1)|} + \ldots + \frac{f_z(z_2)}{|g'(z_2)|} + \ldots + \frac{f_z(z_n)}{|g'(z_n)|} + \ldots \quad (20)$$

$$f_x(x) = \frac{f_z(z_1)}{|g'(z_1)|} + \frac{f_z(z_2)}{|g'(z_2)|}$$

we obtain

$$f_x(x) = \sqrt{\frac{2}{\pi}} \frac{x}{\sqrt{x^2 - l_o^2}} e^{-\frac{1}{2}(x^2 - l_o^2)} \quad (21)$$

which is the modified form of exact $f_x(x)$ in (9) due to approximation of $f_z(z)$ in (13) by a Gaussian. Both pdfs of $f_z(z)$ given by (9) and given by (21) are shown together for comparison in figure 4, where the difference appears to be not significant for this research.
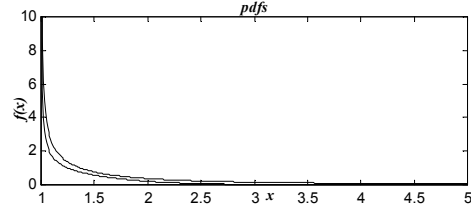

Figure 4: The visual perception pdf $f_x(x)$ and approximation to it (lower) due to Gaussian pdf $f_z(z)$ in figure 2.

The result of the relative importance of the front view as compared to side views in human visual perception can be explained easily as sketched in figure 5.
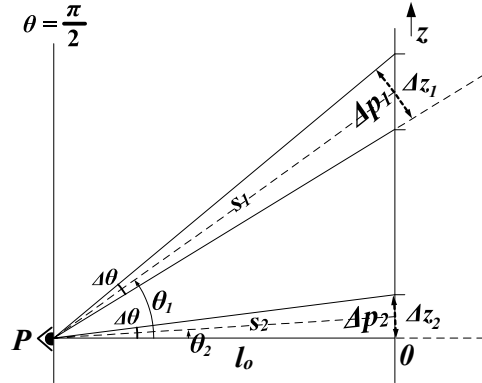

Figure 5: Sketch explaining the relative importance of the viewing direction for visual perception.

In figure 5,

$$\Delta z_1 \cong \frac{\Delta\theta\, s_1}{\cos\theta} \quad, \Delta z_2 \cong \frac{\Delta\theta\, s_2}{\cos\theta}$$

$$s_1 = \frac{l_o}{\cos\theta_1} \quad ; s_2 = \frac{l_o}{\cos\theta_2}, \text{ so that}$$

$$\Delta z_1 \cong \frac{\Delta\theta\, l_o}{\cos^2\theta_1} \quad , \Delta z_2 \cong \frac{\Delta\theta\, l_o}{\cos^2\theta_2}$$

Noting that for $\theta=0$, we obtain

$$\Delta z_2 \cong \Delta\theta\, l_o \quad , \Delta z_1 \cong \frac{\Delta\theta\, l_o}{\cos^2\theta_2} \tag{22}$$

Since $\Delta z_2 < \Delta z_1$, this clearly shows that the visual resolution is higher for the case with θ_2 relative to the case with θ_1. This implies that one gets more visual details at the origin as the visual resolution is higher there and consequently the general shape of pdf $f_z(z)$ exhibits a maximum for θ_2 there, which can be seen in figure 2.

The next step is to move from visual perception to visual openness perception via the sigmoid function. In this case we aim at to find the pdf of the sigmoid function output when the independent variable has the pdf of visual perception given by (10). In this case the theorem on the *function of random variable* can be written as

$$f_y(y) = \frac{f_x(x_1)}{|g'(x_1)|} + ... + \frac{f_x(x_2)}{|g'(x_2)|} + ... + \frac{f_x(x_n)}{|g'(x_n)|} + ... \tag{23}$$

where $f_x(x)$ is given by (7) and $g(x)$ is the sigmoid function given by

$$y = \frac{1}{1+e^{-(x-x_o)}} \tag{24}$$

We use the theorem on the function of random variable given by (23), to obtain the pdf of the visual openness perception. For that matter, first we compute the derivative of $g(x)$ with respect to x where

$$g(x) = \frac{1}{1+e^{-(x-x_o)}} \tag{25}$$

and the derivative is found to be

$$g'(x) = \frac{e^{(x-x_o)}}{[1+e^{-(x-x_o)}]^2} \tag{26}$$

From (25), the root of the equation is obtained as

$$x_1 = \ln\left[\frac{y}{1-y}\right] + x_o \tag{27}$$

Substitution of (27) into (9) gives

$$f_x(x_1) = f_x(y)$$

$$f_x(y) = \frac{4}{\pi\left[\ln\left(\dfrac{y}{1-y}\right)+x_o\right]\sqrt{\left[\ln\left(\dfrac{y}{1-y}\right)+x_o\right]^2 - l_o^2}} \tag{28}$$

$$g'(x_1) = y - y^2 \tag{29}$$

Now, substitution of (28) and (29) into (23), yields

$$f_y(y) = \frac{4}{\pi(y-y^2)\left[\ln\left(\dfrac{y}{1-y}\right)+x_o\right]\sqrt{\left[\ln\left(\dfrac{y}{1-y}\right)+x_o\right]^2 - l_o^2}} \tag{30}$$

for the interval corresponding to $\theta = \pm\pi/2$, in figure 2

$$\frac{1}{1+e^{-(l_o-x_o)}} \leq x \leq \frac{1}{1+e^{-\sqrt{2}\,l_o-x_o}}$$

This is the pdf of the visual openness perception. Variation of this function is shown in figure 6, for $x_o=1$ and $l_o=1$. For this case $0.5000 \leq x \leq 0.6021$.
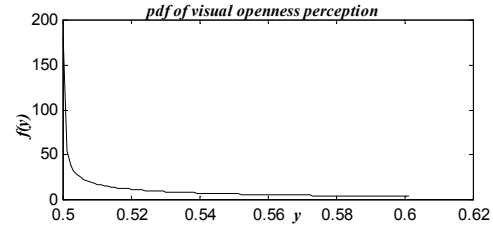
Figure 6: Plot of probability density function of random variable representing the output of the sigmoid function as visual openness perception measurement outcome.

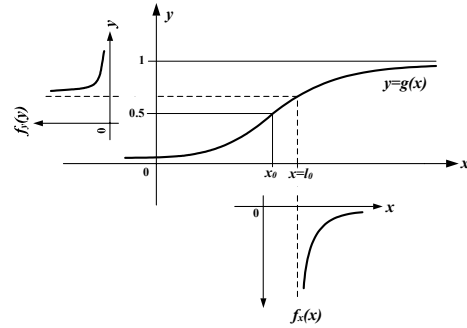The $f_x(x)$ and $f_y(y)$ are depicted together in figure 7 to summarize the probabilistic computations above.

Figure 7: The sketch of both probability density functions of random variables x and y at the sigmoid input and output respectively.

From figure 7, it is seen that, the visual openness perception is also strongly concentrated at the distance $x=l_o$, which is in the direction perpendicular

to the plane, along the axis of the cone in figure 2. This means both visual perception and visual openness perception have similar properties, namely exhibiting maximum concentration along the axis of the visual sight cone. This is what one commonly experiences during the perception of the environment.

To simplify the $f_y(y)$ in (30), we can consider the case where $g(x)$ is approximately linear so that function of a random variable $y=f(x)$ is given by

$$y = a\,x + b \tag{31}$$

In this case the equation $y=ax+b$ has a single solution

$$x = \frac{y-b}{a} \tag{32}$$

for every y. Since $g'(x)=a$, we conclude from (23) that the density of y is given by

$$f_y(y) = \frac{1}{|a|} f_x\left(\frac{y-b}{a}\right) \tag{33}$$

and therefore

$$f_y(y) = \frac{1}{|a|}\,\frac{4}{\pi}\,\frac{1}{\left(\frac{y-b}{a}\right)\sqrt{\left(\frac{y-b}{a}\right)^2 - l_o^2}} \tag{34}$$

Since the sigmoid function can be approximated by three linear functions as local approximations, it is easy to conclude that, the general formulation of $f_y(y)$ as to visual openness perception remains the same having latent dependency to the parameters x_o and l_o, via the parameters a and b in (31), where x_o and l_o are the shift of sigmoid and the distance of the observer to the plane, respectively.

2.2 Determination of the model parameters

For the determination of the parameters in the human visual openness perception model, a vision robot in virtual reality is employed as shown in figure 8. The robot senses its spatial environment by sending rays from its eyes and measuring each length as they hit shapes, which are around the robot. The rays are sent in random directions with a Gaussian pdf as an approximation to $f_z(z)$ given by (13). Formation of Gaussian vision in forward direction with a cone of angle 2θ is sketched in figure 9 where z is the forward direction in the z-x plane. In figure 9, m_z is given by (Ciftcioglu et al., 2006)

$$m_z = (1 + \frac{1}{tg(\theta)})\sqrt{-\ln(2\pi\sigma^2 a^2)} \tag{35}$$

where m_z is the mean in z-direction and $\sigma = \sigma_x = \sigma_z$ is the variance of both Gaussians given by $f_x(x)$ and $f_z(z)$. Note that to have a solution in (35) σ and a must have the condition

$$\sigma^2 a^2 < \frac{1}{2\pi} \tag{36}$$
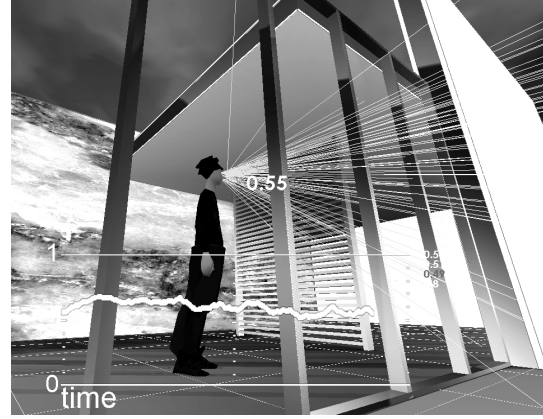
to obtain a real value for m_z.

Figure 8: Virtual perceptual robot viewing environment for visual perception determination. The real-time plot of the perception measurement outcome is indicated.
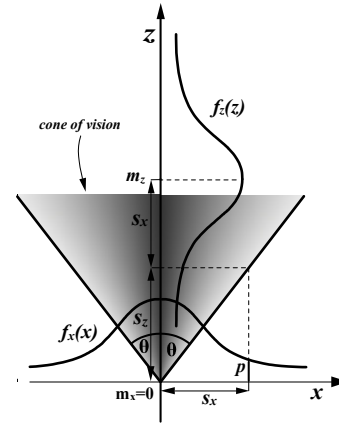

Figure 9: Formation of Gaussian vision in forward direction with a cone of angle 2θ. z is forward direction of the robot in the z-x plane.

The lengths of the rays are converted to virtual openness perception data samples via the sigmoid function, which remains the same throughout the computer experiments. A number of perception data samples are averaged to obtain the degree of visual openness perception of the environment. For this

purpose exponential averaging is used. In exponential averaging previously obtained average information is incorporated into the computation of the current average. By means of this, the average, which is the measurement outcome, is updated in real-time in a computationally efficient and effective way. Greater values for the time constant in exponential averaging yield more accurate measurement outcomes, since more data is used to identify the perception. As a trade off, the time-duration it takes to establish the outcome increases. At the same time the value of the exponentially averaging time-constant determines the accuracy of the measurement outcome in terms of reflecting details of the geometric shape of the perceived space via the pdf of the outcome. The higher the value used for the moving exponential averaging window is, the more accurately shape details of the environment are reflected in the measurement outcome.

Different persons often attribute different degrees of visual openness to the same spatial situation. This indicates that their perceptions are different. To model the perception of individuals as well as to find a standard, jointly valid human perception model is an interesting endeavour from a number of perspectives. For example, in design, requirements for perceptual spatial qualities are generally expressed based on subjective perception. Assessment of requirement satisfaction is a necessary component in the search for optimal spatial shapes, which is an essential activity in architecture and interior design. Another implementation is for robot navigation where the robot uses the common perceptual information about its environment for path planning with humanoid behaviour.

2.2.1 Model identification by means of genetic algorithm

Systematic finding of the appropriate parameter settings of the perception model is essentially an optimality search. Goal of the determination of appropriate model parameters is to maximize the match between modeled perception and human perception. For this purpose a number of perception outcomes are calculated for a selection of spatial scenes, which are also subject to perception assessment by a number of test persons.

Since the visual field is modeled by the random sight lines, the parametric expression of scene cannot be given. That is, although the statistical properties can be analyzed by probabilistic

computation methods using the probability density functions involved, these results cannot be incorporated analytically with the scene for perception assessment. This is due to the visual perception model which receives discrete non-stationary random inputs as granulated elemental perceptions. The stochastic non-stationarity is due to the heterogeneity of the environment that it yields different pdf in the visual perception. In order to be able to handle this non-stationarity imposed on the random inputs, a randomized search method is used, where the discrete nature of the optimization task is also conveniently taken care of. This method is genetic algorithm based optimization, which is employed as shown in Figure 10.
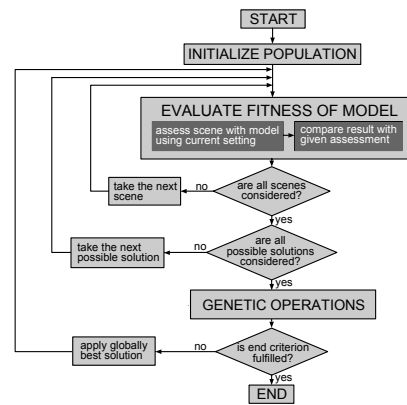

Figure 10: Schematic description of the visual perception model-identification process by means of genetic optimization.

The dataset used to assess the fitness of chromosomes during the genetic evolution are statements of human experimenters regarding their subjective assessment of the visual openness for each scene on a scale from zero to ten. In case of visual openness, ten signifies maximum and zero minimum visual openness. These statements are then normalized to values between 0 and 1 matching the range of the sigmoid function used in the measurement model.

It is noteworthy to stress that genetic optimization has prominent features for this particular measurement system to be able to deal with the non-stationary probabilistic nature of the data samples subject to process and to establish optimality as to actual calibration of the system. By doing so adaptivity is included in the optimization process for other executions involving any additional aspects like spatial complexity, for instance. This can be accomplished conveniently via some modification on the fitting function of the algorithm. After the

genetic evolution the best solutions can be considered as the models of visual openness perception for the test persons.

3   CONCLUSION

The visual perception is investigated and perception of visual openness measurement is presented. The measurement system is established through an associated perception model which is based on probabilistic considerations. The visual openness is measured by means of this probabilistic model. This is most appropriate since the human vision system deals with the natural images using their statistical properties rather than dealing with each piece of image information in order to be able to cope with the complexity of information. For changing scenes, the statistical properties of visual information become non-stationary and the visual process becomes a stochastic process, which is peculiar to this specific research on perception. By means of the model, the characteristic aspects of visual perception are substantiated providing ample insight into the complex visual process.

For the model formation, the method of genetic algorithm is uniquely employed due to the non-stationary nature of the case subject to optimization. The visual openness perception is exercised by a virtual robot having human-like visual perception in a virtual environment with a definitive trajectory, to provide openness assessments as measurement outcomes. Among other applications, such a robot is intended for emulation of human perception providing input for enhanced architectural design. Another important application of common interest is autonomous robotics where the robot moves in an environment without collision by having real-time visual openness perception information during the move without any predefined trajectory. This approach is rather unique as to the novelty of the visual openness perception concept presented here for robotics while a prototype is implemented in virtual reality.

APPENDIX

In the case of circular geometry, the pdf of the visual perception becomes uniform as one intuitively concludes. Referring to figure 2, this is shown mathematically as follows. In circular geometry, the random variable connected to θ is ω where

$$f_\theta(\theta) = 1/(\pi/2)$$

$$\omega = g(\theta) = l_o\theta \tag{A1}$$

$$g'(\theta) = \frac{dg(\theta)}{d\theta} = l_o \tag{A2}$$

Using the theorem on the function of random variable, given by (4) in the text, we write

$$f_\omega(\omega) = \frac{f_\theta(\theta_1)}{|g'(\theta_1)|} \tag{A3}$$

The root of (A1) is given by $\theta_1 = \dfrac{\omega}{l_o}$, which gives

$$f_\omega(\omega) = \frac{2}{\pi\, l_o} \tag{A4}$$

as uniform pdf of visual perception, which satisfies

$$\int_{-l_o\pi/4}^{l\,\pi/4} f(\omega)d\omega = \int_{-l\,\pi/4}^{l_o\pi/4} \frac{2}{\pi\, l_o} d\omega = 1 \quad\text{, as it should be.}$$

REFERENCES

Beetz, M. et al., 2001. Integrated, plan-based control of autonomous robots in Human Environments. In *IEEE Intelligent Systems*. September-October, pp. 2-11.

Ciftcioglu, Ö., Bittermann, M.S. and Sariyildiz, I.S., 2006. Application of a visual perception model in virtual reality. In Proc. *APGV06, Symposium on Applied Perception in Graphics and Visualization, ACM SIGGRAP*. July 28-30, Boston, USA.

Florczyk, S., 2005. *Robot Vision: Video-based Indoor Exploration with Autonomous and Mobile Robot*, Wiley.

Oriolio, G., Ulivi, G. and Vendittelli, M., 1998. Real-time map building and navigation for autonomous robots in unknown environments. In *IEEE Trans. Syst., Man, Cybern. – Part B: Cybernetics*. 28:3, pp. 316-333.

Song, G.B., Cho, S.B., 2000. Combining incrementally evolved neural networks based on cellular automata for complex adaptive behaviours. *ECNN2000, IEEE Symposium on Combinations of Evolutionary Computation and Neural Networks*. May 11-13, San Antonio, TX, USA, pp. 121-129.

Surmann, H., Lingemann, K., Nüchter, A. and Hertzberg, J., 2001. A 3D laser range finder for autonomous mobile robots. In Proc. *32nd Intl. Symp. on Robotics (ISR2001)*. April 19-21, Seoul, Korea, pp. 153-158.

Wang, M., Liu, J. N. K., 2004. On line path searching for autonomous robot navigation. In Proc. *IEEE Robotics, Autom. and Mechatronics*, Singapore, December 1-2, pp. 746-751.